Check for updates

Revising exciton diffusion lengths in polymer dot photocatalysts†

Andjela Brnovic, [ID] Leigh Anna Hunt, [ID] Haining Tian [ID] and Leif Hammarström [ID] *

Exciton migration in organic polymer dots (Pdots) is crucial for optimizing photocatalytic reactions at the particle surface, such as hydrogen evolution and carbon dioxide reduction. Despite the use of Pdots in photocatalysis, there is still a need for better understanding of exciton diffusion within these systems. This study investigates the exciton diffusion in PFBT Pdots stabilized with different weight percentages of the co-polymer surfactant PS–PEG–COOH and doped with perylene red as an internal quencher. Time-resolved fluorescence quenching data yields a quenching volume that the excitons explore during their lifetime (V_q), which is comparable to the volume of the hydrophobic core of PFBT Pdots. This indicates that excitons can migrate to the particle surface with high probability and suggests that the intrinsic exciton diffusion length ($L_D \approx 19$ nm) for PFBT is significantly larger than previously reported in Pdot studies from the literature (5.3 and 8.6 nm). Additionally, a larger quenching rate constant (k_q) and smaller volume (V_q) is observed for the higher PS–PEG–COOH weight ratio, which are attributed to their smaller core. The study provides insights into the exciton migration within Pdots, with important implications for photocatalysis.

Introduction

Organic polymer dots (Pdots) are π-conjugated, semiconducting polymers prepared as nanoparticles with particle size less than 100 nm. They have attracted attention in recent years for the photocatalytic synthesis of solar fuels from water and carbon dioxide.[1–3] Photoexcitation of Pdots results in the formation of tightly bound and localized Frenkel excitons within one of the polymer segments, followed by non-radiative energy transfer between the segments in a series of incoherent hopping steps, a process known as exciton diffusion. Of particular importance in this study is the diffusion of singlet excitons, which is facilitated by Förster resonance energy transfer (FRET).[4–11] In the context of solar photochemistry, the efficiency of light-harvesting relies, among several other factors, on the diffusion of excitons to the Pdots–water interface where photocatalytic reactions take place. The self-assembly of conjugated polymers into Pdots allows them to be effectively dispersed in water where its high dielectric constant promotes dissociation of excitons at the interface.[9,12] Thus, a long exciton diffusion length (L_D), *i.e.*, long-range excitation energy transport, with L_D being at least similar to the Pdot radius is necessary for their optimal photocatalytic performance.[12,13]

Department of Chemistry, Ångström Laboratory, Uppsala University, SE 751 20 Uppsala, Sweden. E-mail: leif.hammarstrom@kemi.uu.se

† Electronic supplementary information (ESI) available. See DOI: https://doi.org/10.1039/d4cp04108a

Accurately measuring exciton diffusion in Pdots, however, has been challenging due to inconsistencies in the existing literature regarding modeling approaches.[14–22] To address this, we used semiconducting polymer PFBT, as it has been intensively investigated for different photocatalytic proton and carbon dioxide reduction reactions in single-component and heterojunction Pdots.[23–26] Additionally, PFBT Pdots have been used previously as a model system to gain better understanding of exciton diffusion in Pdots.[19,21,26] In a study by Groff *et al.*, L_D of PFBT Pdots was investigated through doping with the internal quencher perylene red.[19] The Stern–Volmer analysis of steady-state fluorescence data yielded L_D = 5.3 nm, while simulations incorporating energy transfer quenching by both perylene red and defects in PFBT resulted in L_D = 12 nm for hypothetically defect-free PFBT Pdots. The authors concluded that existing methods for determining L_D experimentally might distort their accurate values, attributing this to quenching by volumetrically distributed defects in aggregated systems such as Pdots. Significant quenching by defects was supported by the much shorter reported average excited state lifetime of PFBT Pdots (0.8 ns) compared to PFBT in a good solvent such as THF (*ca.* 3.0 ns). Building upon this study, Ponzio *et al.* determined L_D of PFBT Pdots through titration with the external quencher rhodamine B.[21] A more detailed theoretical modeling was performed, yielding a L_D value of 8.6 nm, and the quenching by defect sites distributed on the Pdot surface rather than volume was proposed. However, the excited state lifetime of Pdots was reported as *ca.* 2.8 ns, suggesting that the defect

This journal is © the Owner Societies 2025

Phys. Chem. Chem. Phys., 2025, **27**, 1083–1088 | 1083

density was much lower than in Groff *et al.* Agreement between the simulations and experiments was fair, but time-resolved fluorescence data with rhodamine B were lacking, and defect quenching kinetics were poorly fit by the model used.

Here, we use analytical model to fit time-resolved fluorescence data of Pdots to determine the quenching volume (V_q) that the excitons explore during their lifetime and estimate L_D. The model was originally developed independently by Infelta and Tachiya for fluorescence quenching in micelles.[27,28] To our knowledge, this is the first study to utilize the Infelta–Tachiya model for investigating exciton diffusion in Pdots. We use PFBT (average $M_n \leq 25\,000$) Pdots stabilized with different weight ratios of the amphiphilic co-polymer surfactant PS–PEG–COOH (M_w 36 500) (1 : 1 or 1 : 3 PFBT:PS–PEG–COOH (wt/wt)) and doped with perylene red as internal energy transfer quencher (Förster radius R_0 = 3 nm (ref. 19)) distributed within the hydrophobic core of the particle. PS–PEG–COOH provides electrostatic and steric stabilization to the particles surface, ensures colloidal stability, and is not photo- or redox active.[24,29] From time-resolved fluorescence decay traces at different quencher concentrations, we estimated V_q and the rate constant for quenching in the exciton volume (k_q).

Results and discussion

Pdots were prepared by a nanoprecipitation method, with different concentrations of the quencher perylene red (a detailed procedure is provided in the ESI†).[2,24] Chemical structures of PFBT, perylene red, and PS–PEG–COOH are presented in Fig. 1. The quencher was assumed to be randomly distributed within the hydrophobic particle core, as both the excited probe (PFBT) and the quencher have hydrophobic properties. The hydrodynamic radii of PFBT Pdots were determined using dynamic light scattering (DLS) (Fig. S1a and b, ESI†). Both single-component PFBT and doped PFBT Pdots had an average radius of 15 nm for both 1 : 1 or 1 : 3 (wt/wt) ratios, which suggests that the number of Pdots per volume in the latter solution was larger for the same concentration of PFBT. PS–PEG–COOH has stabilizing properties in colloids where its sterically demanding PEG groups prevent aggregation. We suggest that the higher PS–PEG–COOH content likely favoured the formation of smaller Pdots with increased surface curvature, as it provided larger volume per PEG chain. Thus, instead of forming larger Pdots at the 1 : 3 (wt/wt) ratio, the core volume decreased, maintaining a hydrodynamic radius comparable to that of the 1 : 1 (wt/wt) ratio. The UV-Vis absorption spectra of Pdots
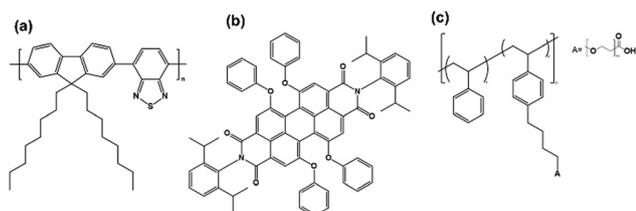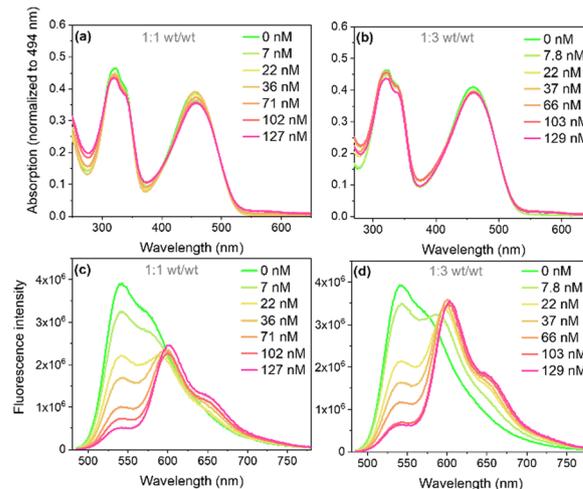

Fig. 2 Absorption (a) and (b) and fluorescence (c) and (d) spectra with excitation at 473 nm (Abs = 0.08) of single-component and doped PFBT Pdots at 1 : 1 and 1 : 3 (wt/wt) ratios.

(Fig. 2a and b) showed broad absorption extending into the visible region up to 540 nm, with two distinct absorption bands at ~310 nm and ~470 nm. Upon doping with perylene red, a weak, red-shifted absorption band appeared between 550 and 620 nm, corresponding to perylene red absorption (Fig. S2, ESI†) and showed a steady increase with increasing perylene red concentration. The doping concentrations of perylene red used were 7, 22, 36, 71, 102, and 127 nM for the 1 : 1 (wt/wt) ratio, and 7.8, 22, 37, 66, 103, and 129 nM for the 1 : 3 (wt/wt) ratio, determined from the amount of perylene red added during Pdots preparation.

The steady state fluorescence spectra of PFBT and doped PFBT Pdots under selective excitation of PFBT at 473 nm is shown in Fig. 2c and d. The PFBT fluorescence peak at 540 nm decreased with increasing perylene red concentration, while an additional fluorescence band from perylene red appeared with a peak at 600 nm and a shoulder around 660 nm (*cf.* Fig. S2, ESI†), which suggests FRET between PFBT and perylene red within Pdots. The occurrence of energy transfer was supported by overlaying the corrected excitation spectra for perylene red emission onto the absorption spectra of doped PFBT Pdots (Fig. S3, ESI†).

Time-resolved fluorescence measurements revealed that the decrease in fluorescence emission of PFBT in the presence of perylene red was followed by a near equivalent reduction of fluorescence lifetime, which is consistent with dynamic (diffusional) quenching (Fig. 3a and b). Fluorescence decay traces of PFBT Pdots with no quencher present were fit with a double-exponential decay function with time constants of τ_1 = 1.4 ns (A_1 = 0.76) and τ_2 = 3.4 ns (A_2 = 0.24) for 1 : 1 (wt/wt) ratio and of τ_1 = 1.3 ns (A_1 = 0.76) and τ_2 = 3.6 ns (A_2 = 0.24) for 1 : 3 (wt/wt) ratio. The double-exponential behavior suggests inhomogeneous probe environments. In contrast to PFBT dissolved in THF, where polymeric chains are isolated by solvent molecules and exhibit a single exponential fluorescence decay with an excited state lifetime of 2.8 ns (Fig. S4, ESI†), the polymeric chains in Pdots are densely packed.
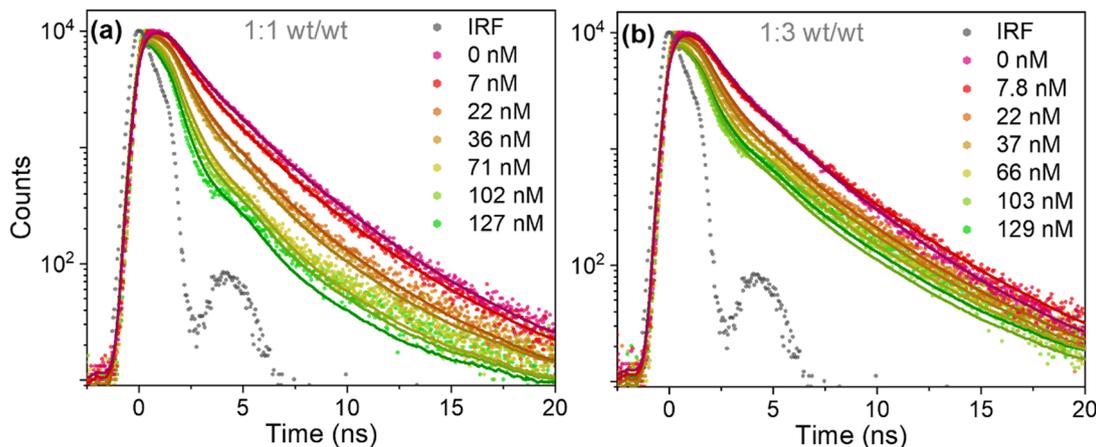

Fig. 1 Chemical structures of (a) PFBT, (b) perylene red and (c) PS–PEG–COOH.

1084 | *Phys. Chem. Chem. Phys.*, 2025, **27**, 1083–1088

This journal is © the Owner Societies 2025

Fig. 3 Fluorescence decay traces of PFBT Pdots at different quencher concentrations, at 1:1 (a) and 1:3 (b) (wt/wt) ratios. The fits according to eqn (1) are convoluted with the IRF, with freely adjustable k_q and $\langle n \rangle$ parameters.

The fluorescence lifetimes were reduced as the perylene red concentration was increased (Fig. 3a and b). Fluorescence decay traces of doped PFBT Pdots were well described by the Infelta–Tachiya model (eqn (1)),[27,28] that in its original form has been employed to describe fluorescence quenching kinetics in micellar solutions. The model assumes a random (Poisson) distribution of quenchers over the Pdots and in its simplest form, which is appropriate here, assumes no migration of excitons or quenchers between the particles. An important difference to micelles is that the Pdot volume can be larger than the exciton quenching volume, *i.e.* the volume the exciton can explore during its lifetime. Only excitons that contain a quencher within its V_q will be quenched, and the quenching is faster the more quenchers that are in the volume. In eqn (1), we use a sum of two Infelta–Tachiya terms to account for the biexponential decay behavior of the Pdots fluorescence in the absence of quenchers:

$$I(t,n,k_q) = A_1 \cdot \exp(-k_1 \cdot t + \langle n \rangle \cdot (\exp(-k_q \cdot t) - 1))$$
$$+ A_2 \cdot \exp(-k_2 \cdot t + \langle n \rangle \cdot (\exp(-k_q \cdot t) - 1)) \quad (1)$$

Here, $k_1 \left(k_1 = \frac{1}{\tau_1} \right)$ and $k_2 \left(k_2 = \frac{1}{\tau_2} \right)$ are rate constants for the sample without added quencher and their relative amplitudes A_1 and A_2, n is the average number of quenchers per V_q, and k_q is the first-order quenching rate constant for quenching in volumes with at least one quencher. To obtain robust fits, the value of k_q was assumed to be the same in both terms.

Firstly, single trace fits were performed according to eqn (1) with all parameters freely adjustable, as shown in Fig. 3a and b (solid line). Here, the values of k_1, k_2, A_1 and A_2 were fixed to their values in the absence of quenchers, while k_q and n were floating parameters. The values of k_q and n obtained for different perylene red doping concentrations are summarized in Table 1. With increasing doping concentrations above 40 nM, n increased much less than proportionally with concentration and k_q increased. This deviation from the model could be attributed to the perylene red aggregated species formation when there is more than one quencher per Pdot present.[19,30]

Table 1 Fluorescence decay parameters obtained from single trace and global fitting

	Perylene red/nM	Single trace fitting		Global fitting	
		k_q/ns^{-1}	$\langle n \rangle$	k_q/ns^{-1}	$\langle n \rangle$
1:1 (wt/wt) Pdots	7.2	0.37	0.4	0.47	0.3
	22	0.42	1.1	0.47	1
	36	0.47	1.4	0.47	1.3
	71	0.57	2.2	—	—
	102	0.67	2.4	—	—
	127	0.77	2.7	—	—
1:3 (wt/wt) Pdots	7.8	0.75	0.15	0.89	0.084
	22	0.73	0.77	0.89	0.71
	37	0.86	0.97	0.89	0.91
	66	1.2	1.2	—	—
	103	1.3	1.6	—	—
	129	1.4	1.5	—	—

Aggregation can also explain why the perylene red fluorescence intensity in Fig. 2c and d did not increase after 40 nM was reached, although the PFBT fluorescence was further quenched.

For the global fit analysis, we used only the data with <40 nM quencher, where aggregation effects should be small and k_q invariant with quencher concentration as expected in the Infelta–Tachiya model (Fig. 4b and c). The fluorescence decay parameters k_1, k_2, A_1, and A_2 were fixed to values obtained from the double-exponential fitting of PFBT Pdots without a quencher. The assessment of the goodness of the fit to the model was based on the weighted residuals. The residuals showed some deviation (only <5 cps compared to 10^4 in the maximum channel) at <5 ns and were randomly distributed around zero for both 1:1 and 1:3 (wt/wt) ratios (Fig. 4d and e). From the values of n obtained and the estimated number of moles of quencher added, we calculated the number of quenching volumes in the sample. With the known mass of PFBT in the sample and its corresponding density, we could then calculate the value of V_q (see ESI†). From the global fit results in Table 1, we calculated V_q values as 2300 nm³ and 1400 nm³, corresponding to spheres with radii of 8.2 nm and 6.9 nm for the 1:1 and 1:3 (wt/wt) ratios, respectively. The hydrodynamic

This journal is © the Owner Societies 2025

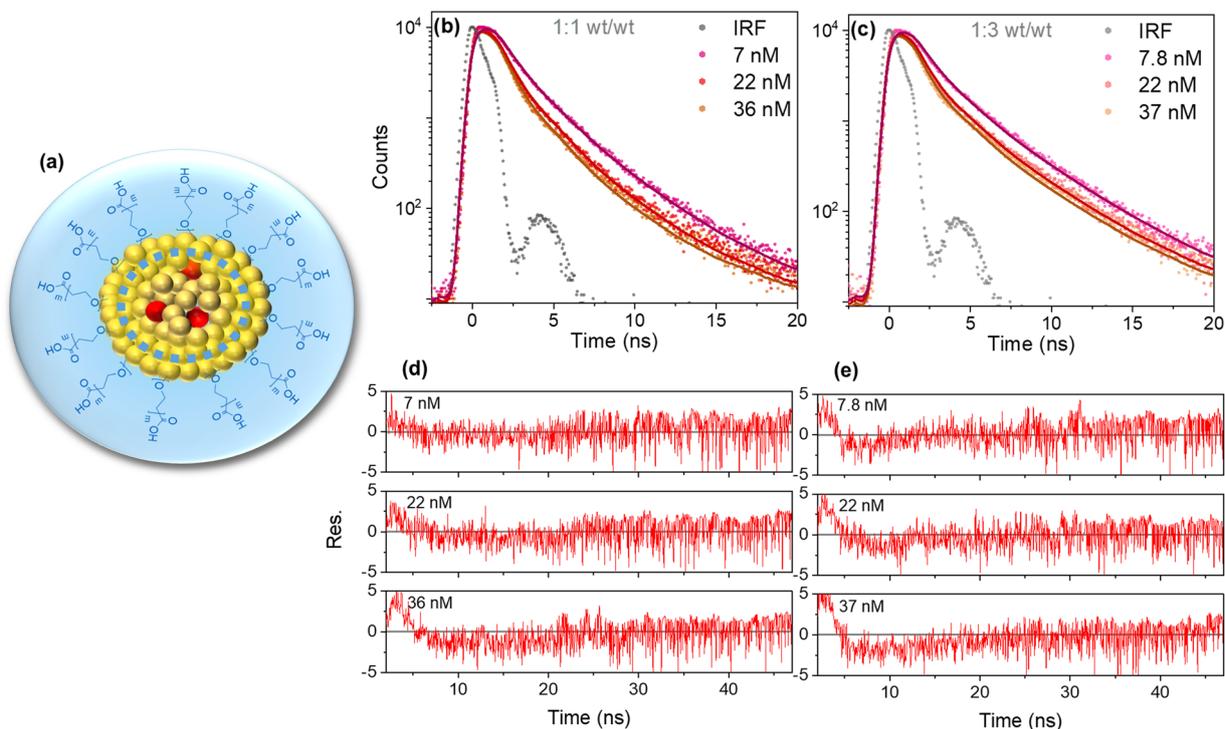*Phys. Chem. Chem. Phys.*, 2025, **27**, 1083–1088 | **1085**

Fig. 4 Illustration depicting the proposed morphology of Pdots for 1:1 and 1:3 (wt/wt) ratio. The dashed blue circle indicates the reduction in V_q for PFBT Pdots at 1:3 (wt/wt) ratio (a). Fluorescence decay traces for three different doping concentrations of PFBT Pdots at 1:1 (b) and 1:3 (c) (wt/wt) ratios convoluted with IRF and globally fit with eqn (1) and their corresponding residuals (d and e).

radii from DLS (15 nm for both (wt/wt) ratios, Fig. S1a and b, ESI†) were larger because DLS captures not only the hydrophobic core but also included the PS–PEG–COOH shell and a solvent layer of certain thickness (Fig. 4a). A precise estimate of the shell thickness is not available, but the molecular weights of the PFBT and the PEG-part of PS–PEG–COOH are very similar (*ca.* 24 000 g mol^{-1}; see ESI†) while the PS-part is smaller (8500 g mol^{-1}). As the PEG-layer is much less dense than the core, it will constitute a major part of the particle volume even for the 1:1 (wt/wt) ratio Pdots. Thus, a conservative estimate of the core radius in the 1:1(wt/wt) Pdots is <75% of the 15 nm value (<42% of the volume), *i.e.* <10.5 nm. Thus, it is likely that the observed V_q is actually limited by the physical size of the hydrophobic core.

The larger k_q values obtained as PFBT is diluted with more PS–PEG–COOH was initially surprising, as it could instead be expected to lead to longer exciton hoping distances and slower quenching. It is not likely to be due to less energetic heterogeneity, as the absorption and fluorescence spectra are essentially identical for the two samples. Instead, the difference in k_q can be attributed to a smaller core volume with the 1:3 (wt/wt) ratio, since the particle size did not change when the concentration of PS–PEG–COOH used for preparation was increased and thus the Pdots concentration must have increased for the same amount of PFBT (Fig. S1a and b, ESI†). Fig. 4a illustrates the proposed reduction in V_q and Pdots morphology. The larger k_q with more PS–PEG–COOH can also explain the similar extent of quenching at similar perylene red concentrations in Fig. 2c and d, although the number of Pdots

is larger and thus n is smaller. The smaller V_q obtained with the 1:3 ratio, in spite of a larger k_q, is also consistent with V_q being limited by the physical size of the hydrophobic cores.

Fluorescence quenching efficiencies from steady-state data were compared with those from the integrated surface areas under the decay curves from time-resolved fluorescence measurements at both (wt/wt) ratios (Fig. 5a and b). The integrated surface areas under the normalized decay curves were estimated from the average lifetimes obtained from eqn (S1) (ESI†) for undoped and eqn (1) for doped Pdots. Steady-state and time-resolved experiments yielded very similar extent of quenching showing that static quenching (not resolved by TCSPC) is less important. Nevertheless, the somewhat larger steady-state intensity quenching suggests that n, and thus V_q, are somewhat
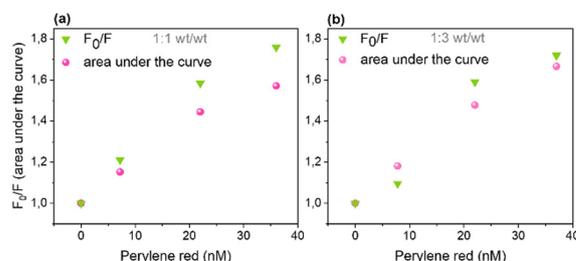

Fig. 5 Comparing fluorescence quenching efficiencies from steady-state data with that from the integrated surface area under the decay curves from time-resolved fluorescence measurements at 1:1 (a) and 1:3 (b) (wt/wt) ratios.

1086 | *Phys. Chem. Chem. Phys.*, 2025, **27**, 1083–1088

This journal is © the Owner Societies 2025

underestimated. It is important to highlight that both Pdots without and with quenchers (>36 nM) contribute significantly to the observed fluorescence as Pdots with quenchers only exhibit moderate quenching. This is different from the model of complete quenching within a sphere-of-action, where the fluorescence intensity ratio *versus* concentration plot shows characteristic upward exponential increase.[31]

Conclusions

In summary, our study uses the Infelta–Tachiya model for fluorescence quenching in particles to provide a new analysis and understanding of exciton migration within PFBT Pdots stabilized with different (wt/wt) ratios of PS–PEG–COOH. In contrast to previous work on PBFT Pdots that have used numerical simulations of steady-state fluorescence intensity data, we use an analytical expression to fit time-resolved fluorescence data. The model's applicability was further confirmed by agreement from both steady-state and time-resolved fluorescence experiments. The estimated V_q value of 2300 nm^3 for 1 : 1 (wt/wt) PBFT : PS–PEG–COOH Pdots, to a spherical radius of 8.2 nm, is similar to the estimated radius of the hydrophobic core, and agrees well with $L_D = 8.6$ nm reported by Ponzio *et al.* using the external quencher rhodamine B.[21] However, our results suggest a significantly longer L_D than that, for the following reasons: (1) the value of V_q obtained in the present study seems to be limited by the radius of the hydrophobic core, as discussed above; and (2) the random walk of excitons with $L_D = \sqrt{\langle x^2 \rangle}$ (r.m.s. displacement in three dimensions) explores a volume much smaller than that of a sphere with radius = L_D. The volume explored by random walk, using the Förster radius (3.0 nm) as the reaction radius, corresponds to the so-called Wiener sausage volume.[32] This suggests that the value of L_D is at least twice the radius of our particle core, $L_D \approx 19$ nm (see ESI† for details), similar to the value estimated from Monte Carlo simulations of neat PFBT thin films (16 nm).[33]

Our results suggest that excitons diffuse to the Pdot surface with high probability, which in addition to their porous properties,[34] are important for photocatalytic applications. This contrasts with light-emitting diode applications, where the exciton diffusion to the particle surface is not required. Moreover, quenching by surface defects, as suggested by Ponzio *et al.*,[21] could be outcompeted by a rapid catalytic reaction. Finally, as excitons diffuse to the Pdot surface to a high extent, we hypothesize that using PS–PEG–COOH could potentially reduce overall defect density, which is supported by the comparable lifetimes between PFBT Pdots in water and PFBT in THF. The study contributes valuable insights into the dynamics of exciton migration and quenching behavior within Pdots, enhancing our understanding for potential applications in energy conversion.

Author contributions

AB and LAH: investigation, formal analysis, validation, writing review and editing. AB: writing original draft. LH and HT:

conceptualization, project administration, supervision, writing review and editing.

Data availability

Data available on request from the authors.

Conflicts of interest

There are no conflicts to declare.

Acknowledgements

Notes and references

1 M. V. Pavliuk, S. Wrede, A. Liu, A. Brnovic, S. Wang, M. Axelsson and H. Tian, Preparation, Characterization, Evaluation and Mechanistic Study of Organic Polymer Nano-Photocatalysts for Solar Fuel Production, *Chem. Soc. Rev.*, 2022, **51**, 6909–6935.

2 L. Wang, R. Fernández-Terán, L. Zhang, D. L. A. Fernandes, L. Tian, H. Chen and H. Tian, Organic Polymer Dots as Photocatalysts for Visible Light-Driven Hydrogen Generation, *Angew. Chem.*, 2016, **128**, 12494–12498.

3 P. J. Tseng, C. L. Chang, Y. H. Chan, L. Y. Ting, P. Y. Chen, C. H. Liao, M. L. Tsai and H. H. Chou, Design and Synthesis of Cycloplatinated Polymer Dots as Photocatalysts for Visible-Light-Driven Hydrogen Evolution, *ACS Catal.*, 2018, **8**, 7766–7772.

4 S. Bhattacharyya, B. Paramanik and A. Patra, Energy Transfer and Confined Motion of Dyes Trapped in Semiconducting Conjugated Polymer Nanoparticles, *J. Phys. Chem. C*, 2011, **115**, 20832–20839.

5 S. Grigalevicius, M. Forster, S. Ellinger, K. Landfester and U. Scherf, Excitation Energy Transfer from Semi-Conducting Polymer Nanoparticles to Surface-Bound Fluorescent Dyes, *Macromol. Rapid Commun.*, 2006, **27**, 200–202.

6 G. D. Scholes, G. R. Fleming, A. Olaya-Castro and R. Van Grondelle, Lessons from Nature about Solar Light Harvesting, *Nat. Chem.*, 2011, **3**, 763–774.

7 G. D. Scholes, Long-Range Resonance Energy Transfer in Molecular Systems, *Annu. Rev. Phys. Chem.*, 2003, **54**, 57–87.

8 O. V. Mikhnenko, P. W. M. Blom and T. Q. Nguyen, Exciton Diffusion in Organic Semiconductors, *Energy Environ. Sci.*, 2015, **8**, 1867–1888.

9 G. D. Scholes and G. Rumbles, Excitons in Nanoscale Systems, *Nat. Mater.*, 2006, **5**, 683–696.

10 B. Jana, A. Ghosh and A. Patra, Photon Harvesting in Conjugated Polymer-Based Functional Nanoparticles, *J. Phys. Chem. Lett.*, 2017, **8**, 4608–4620.

11 T. Förster, Zwischenmolekulare Energiewanderung Und Fluoreszenz, *Ann. Phys.*, 1948, **437**, 55–75.

12 M. Rahman, H. Tian and T. Edvinsson, Revisiting the Limiting Factors for Overall Water-Splitting on Organic Photocatalysts, *Angew. Chem., Int. Ed.*, 2020, **59**, 16278–16293.

13 S. Kundu and A. Patra, Nanoscale Strategies for Light Harvesting, *Chem. Rev.*, 2017, **117**, 712–757.

14 X. Wang, L. C. Groff and J. D. McNeill, Multiple Energy Transfer Dynamics in Blended Conjugated Polymer Nanoparticles, *J. Phys. Chem. C*, 2014, **118**, 25731–25739.

15 K. Lix, K. D. Krause, H. Kim and W. R. Algar, Investigation of the Energy Transfer Mechanism between Semiconducting Polymer Dots and Organic Dyes, *J. Phys. Chem. C*, 2020, **124**, 17387–17400.

16 S. Wang, A. Thorn and G. Redmond, Photophysical Probing of Dye Microenvironment, Diffusion Dynamics, and Energy Transfer, *J. Phys. Chem. C*, 2018, **122**, 6900–6911.

17 J. A. Bjorgaard and M. E. Köse, Amplified Quenching of Conjugated Polymer Nanoparticle Photoluminescence for Robust Measurement of Exciton Diffusion Length, *J. Appl. Phys.*, 2013, **113**, 203707.

18 K. Trofymchuk, L. Prodi, A. Reisch, Y. Mély, K. Altenhöner, J. Mattay and A. S. Klymchenko, Exploiting Fast Exciton Diffusion in Dye-Doped Polymer Nanoparticles to Engineer Efficient Photoswitching, *J. Phys. Chem. Lett.*, 2015, **6**, 2259–2264.

19 L. C. Groff, X. Wang and J. D. McNeill, Measurement of Exciton Transport in Conjugated Polymer Nanoparticles, *J. Phys. Chem. C*, 2013, **117**, 25748–25755.

20 A. Ghosh, B. Jana, A. Kumar, S. Ghosh and A. Patra, Manipulation of the Exciton Diffusion Length of Conjugated Polymer Nanoparticles: Role of Electron and Hole Scavenger Molecules, *Bull. Mater. Sci.*, 2020, **43**, 174.

21 R. A. Ponzio, R. M. Spada, A. B. Wendel, M. V. Forcone, F. D. Stefani, C. A. Chesta and R. E. Palacios, Exciton Diffusion, Antenna Effect, and Quenching Defects in Superficially Dye-Doped Conjugated Polymer Nanoparticles, *J. Phys. Chem. C*, 2021, **125**, 23299–23312.

22 C. Wu, Y. Zheng, C. Szymanski and J. D. McNeill, Energy Transfer in a Nanoscale Multichromophoric System: Fluorescent Dye-Doped Conjugated Polymer Nanoparticles, *J. Phys. Chem. C*, 2008, **112**, 1772–1781.

23 L. Wang, R. Fernández-Terán, L. Zhang, D. L. A. Fernandes, L. Tian, H. Chen and H. Tian, Organic Polymer Dots as Photocatalysts for Visible Light-Driven Hydrogen Generation, *Angew. Chem., Int. Ed.*, 2016, **55**, 12306–12310.

24 A. Liu, L. Gedda, M. Axelsson, M. V. Pavliuk, K. Edwards, L. Hammarström and H. Tian, Panchromatic Ternary Polymer Dots Involving Sub-Picosecond Energy and Charge Transfer for Efficient and Stable Photocatalytic Hydrogen Evolution, *J. Am. Chem. Soc.*, 2021, **143**, 2875–2885.

25 B. Cai, M. Axelsson, S. Zhan, M. V. Pavliuk, S. Wang, J. Li and H. Tian, Organic Polymer Dots Photocatalyze CO2 Reduction in Aqueous Solution, *Angew. Chem., Int. Ed.*, 2023, **135**, e202312276.

26 M. Sachs, H. Cha, J. Kosco, C. M. Aitchison, L. Francàs, S. Corby, C. L. Chiang, A. A. Wilson, R. Godin, A. Fahey-Williams, A. I. Cooper, R. S. Sprick, I. McCulloch and J. R. Durrant, Tracking Charge Transfer to Residual Metal Clusters in Conjugated Polymers for Photocatalytic Hydrogen Evolution, *J. Am. Chem. Soc.*, 2020, **142**, 14574–14587.

27 M. Tachiya, Application of a Generating Function to Reaction Kinetics of Quenching of Luminescent Probes in Micelles, *Chem. Phys. Lett.*, 1975, **33**, 289.

28 P. P. Infelta, M. Gratzel and J. K. Thomas, Luminescence Decay of Hydrophobic Molecules Solubilized in Aqueous Micellar Systems A Kinetic Model, *J. Phys. Chem.*, 1973, **78**, 190–195.

29 A. Brnovic, L. Hammarström and H. Tian, Mechanistic Insights into the Photocatalytic Hydrogen Production of Y5 and Y6 Nanoparticles, *J. Phys. Chem. C*, 2023, **127**, 12631–12639.

30 F. Würthner, Perylene Bisimide Dyes as Versatile Building Blocks for Functional Supramolecular Architectures, *Chem. Commun.*, 2004, 1564–1579.

31 J. R. Lakowicz, *Principles of Fluorescence Spectroscopy*, Springer, US, Boston, MA, 2006.

32 A. M. Berezhkovskii, Yu. A. Makhnovskii and R. A. Suris, Wiener Sausage Volume Moments, *J. Stat. Phys.*, 1989, **57**, 333–346.

33 S. Westenhoff, I. A. Howard and R. H. Friend, Probing the Morphology and Energy Landscape of Blends of Conjugated Polymers with Sub-10 nm, Resolution, *Phys. Rev. Lett.*, 2008, **101**, 016102.

34 A. Liu, C. W. Tai, K. Holá and H. Tian, Hollow Polymer Dots: Nature-Mimicking Architecture for Efficient Photocatalytic Hydrogen Evolution Reaction, *J. Mater. Chem. A*, 2019, **7**, 4797–4803.

1088 | *Phys. Chem. Chem. Phys.*, 2025, **27**, 1083–1088

This journal is © the Owner Societies 2025